Journal of Interdisciplinary Mathematics
ISSN: 0972-0502 (Print), ISSN: 2169-012X (Online)
Vol. 26 (2023), No. 2, pp. 201–229
DOI : 10.47974/JIM-1420

Dynamics and control of a mathematical delayed Cholera model

Adamu Shitu Hassan *
Justin M. W. Munganga †
Department of Mathematical Sciences
University of South Africa
Florida Science Campus
Johannesburg
South Africa

Abstract

A delay differential equation-cholera model with infection from aquatic reservoir and environmental disinfection as intervention is constructed and analyzed in human population. It is assumed that the time lag is the period between oral intake of contaminated water or food to full cholera infection in the population. Basic properties of the model that ascertain its mathematical and epidemiological well-posedness are determined. A unique disease-free and cholera endemic equilibria are found and the control reproduction number is computed. Global and local attractiveness for disease-free and endemic equilibria are proved to depend on the control reproduction number and time delay as threshold quantities. The impacts of time delay on stability of equilibria and endemicity are studied, furthermore conditions for Hopf bifurcation are computed. Disinfection of environment is shown to increase the number of healthy individuals and lower the concentration of cholera in the environment. Numerical simulations are used to support theoretical results.

Subject Classification: *37N25, 37N30, 92B05.*

Keywords: *Cholera, Delay, Aquatic environment, Hopf bifurcation, Disinfection.*

1. Introduction

Cholera is an acute watery diarrhoeal infection for small intestine in humans caused by the bacterium *Vibro cholerae* (*V. cholerae*) that can result in

* *E-mail:* **hashitu.mth@buk.edu.ng; shituha@unisa.ac.za (Corresponding Author)**
† *E-mail:* **munganjwa@unisa.ac.za**

© Taru Publications

death within hours if left untreated. It becomes a substantial public health problem in developing countries, especially internally displaced camps and flood areas that lack sufficient access to clean water and sanitation facilities [48]. Most of cholera infected individuals don't show any sign of ailment, and the microbes can stay in their defecation for 1 – 10 days after infection and are shed once again into aquatic surrounding, possibly infecting other individuals [49]. The first cholera outbreak occurred in the Bay of Bengal in 1817 – 1824 [36]. Subsequently, cholera outbreaks were reported to emerge and re-emerge in Congo (2008), Vietnam (2009), Nigeria (2005 – 2009), Zimbabwe (2008) and Haiti (2010) [30, 47]. Recently, (up to 22 October 2021), many African and Asian countries have recorded cholera epidemics as reported in [12]. For instance, in Africa, 8,433,885 cases are reported with majority of cases from South Africa (2,916,593), Morocco (942,132), Tunisia (710,953), Ethiopia (359,247) and Libya (350,628). The total cholera deaths reported from Africa stand at 215,449 with most deaths from South Africa (88,612), Tunisia (25,100), Egypt (17,970), Morocco (14,544) and Ethiopia (6,217). Globally, it has been reported that cholera affects 2.9 million people causing a total of 95,000 fatal cases annually [16]. Cholera and indeed other infectious diseases tend to be global threats to community health and indicators of inadquate social amenities and poverty [3, 8, 37, 40, 42].

The most prominent transmission of cholera in humans is through indirect path from environments by uptake of contaminated water or food with *V. cholerae* bacteria [9, 15]. According to physiological studies, it was revealed that toxigenic *V. cholerae* can florish in some aquatic habitats associated with zooplankton and other organisms from two months to years with possible reinfection of the environment [10]. Furthermore, in [2], it has been stated that *V. cholerae* is a natural inhabitant of brackish riverine, estuarine, and coastal waters. In a recent study conducted in Bepanda, Cameroon, cholera pathogens are present in wells and streams all year round [1]. Other less probable direct transmission path also exists, when humans ingest water or food contaminated directly by other humans infected with *V. cholerae* [30, 31].

The noticeable indicators of cholera are vomiting, watery diarrhoea, loss of skin elasticity and severe dehydration [54]. The time period from infection to appearance of symptoms for cholera is between few hours to 5 days [28, 35]. Supply of safe water, rehydration therapy, proper waste management, effective sanitation/personal hygiene and vaccination are critical to prevent and control the transmission of cholera and other water-borne diseases [6, 49, 51]. Cholera affects all age groups (children and

adults) and can lead to death quickly if neglected, as in the case of other communicable diseases [5, 49].

Mathematical modelling of cholera has explored the knowledge in understanding the mechanisms involved in transmission, control and suggesting optimal strategies. In particular, the cholera model developed by Capasso and Paveri-Fontana [7], consists of infected humans and bacteria populations in the sea. The model of [7] was later extended by Code¸co [9], by adding a susceptible human population to study the long term dynamics. In order to assess the impact of incubation period, Wang and Wei [44], studied the global dynamics of the model in [9] with time delay in the infected humans as they contribute to the cholera in the environment. Later, Misra *et al.* [28], considered the effect of time delay in controlling the carrier dependent cholera epidemics. To explore the contribution of environment in cholera infection, Zhou *et al.* [51] considered stability and backward bifurcation on a cholera model with saturated recovery rate with infection only from the environment. Furthermore, the role of bacteriophage viruses in aquatic reservoirs was studied by Misra *et al.* [27] by formulating a model that combines models proposed by Code¸co [9] and that of Beretta and Kuang [4].

It is well known fact that cholera epidemic spreads more rapidly in human population due to oral ingestion of *V. cholerae* found in contaminated water or food than human to human transmission. Thus, to prevent the prevalence of cholera outbreak, eradication of pathogenic cholera from contaminated environment by spraying disinfectant may be an excellent control strategy that kills bacteria or inhibit their growth in the aquatic environment [13]. Usually, the infection is not immediate, there is a time lag between oral intake to full cholera infection, which may be a determining factor for model dynamics and/or controlling cholera epidemic. Motivated by the old history of *V. cholerae* in aquatic environment [9, 15, 36], effect of time delay in the spread of cholera and use of disinfectant in the habitat as control strategy, in this work we formulate and analyze a delay differential equation model for cholera infection from aquatic reservoir only and consider the disinfection of environment as intervention. In this case, the time delay is the period between oral intake of contaminated water or food to full cholera infection in the population. The objective is to see how time delay can affect the inhibition of cholera pathogens by susceptibles to become infectious and determine conditions for Hopf bifurcation with delay as the parameter. Furthermore, the study will determine the influence of environmental disinfection as control strategy of cholera in the population.

The remaining part of the paper is organized as follows. In Section 2, the model formulation is presented, and preliminary results are presented in Section 3. Stability analysis of equilibria and computation of control reproduction number are presented in Section 4. Numerical analysis and effects of control strategy are considered in Section 5. Finally, a conclusion is given in Section 6.

2. Model formulation

A compartmental delay differential equations model is formulated consisting of human population and *V. cholerae*, in aquatic environment. The human population at time t, is divided into three non- intersecting classes: the susceptibles $S(t)$, are the healthy individuals that can get infected by ingestion of contaminated food or water from the environment; infectious individuals $I(t)$, the individuals who are infected and can spread *V. cholerae*, and the recovered individuals $R(t)$, those that regain health by acquiring natural immunity and due to disinfection of cholera in the environment. Taking into account the immunity loss by recovered humans that occur in the real life situation, the recovered individuals become susceptible. However, here we assume that natural immunity combine with the disinfection of environment will result in long immunity, so $R(t)$ may not revert to $S(t)$ immediately. Infectious recover at rate γ, shedding cholera bacterium to aquatic environment at rate ξ, and dying due to cholera infection and naturally at rates μ and δ, respectively. The total human population $N(t)$, is therefore given by $N(t) = S(t) + I(t) + R(t)$. The concentration of *V. cholorae* in aquatic environment at time t, is denoted by $B(t)$. We consider a delay $\tau \geq 0$ that represents the time between oral intake of contaminated water or food by susceptibles to full cholera infection in the population. For incidence functions in susceptible and infectious sub-populations, we use the formulations in [20, 24, 46] and the modified Michaelis-Menten saturated incidence function as follows:

(1) The incidence function is given by $\frac{\beta_e B(t)}{\kappa + B(t)} S(t)$, where β_e is the sufficient ingestion rate of contaminated food/water from the aquatic reservoir that can lead to cholera infection. The constant $\kappa > 0$, is the half-saturation rate of *V. cholerae* in an aquatic environment that can lead to 50% cholera infection.

(2) The susceptibles are infected with time lag τ times ago $(t - \tau)$ as a result of ingesting pathogenic cholera and become infectious at

current time t, so that the number of newly infectious human is $\frac{\beta_e B(t-\tau)S(t-\tau)e^{-\mu\tau}}{\kappa + B(t-\tau)}$ provided that they survive natural death with survival probability $e^{-\mu\tau}$ through the period $[t-\tau, t]$.

Cholera pathogens decay naturally or as a result of disinfection of environment at a rate η while the aquatic environment is disinfected at rate ν as a control measure. The model equations given in (1)–(4), initial functions (5) and the schematic diagram in Figure 1 describe the model, where $\lambda_e \frac{\beta_e B(t)}{\kappa + B(t)} S(t)$ represents the incidence function in (1). Since the model concerns about biological populations, all parameters of the model are positive at all times. This work extends some of the existing studies for cholera and other water borne disease transmissions in the literature; in particular, those presented in [9, 29, 38, 51] as follows.

(i) In [9], no time delay and control strategy were used.

(ii) In [29], they used simple mass action formulation as against the realistic standard incidence formulation.

(iii) In [38, 51], no time delay was used.

The compartmental model in Figure 1 is written as a system of delay differential equations given by the system.

$$\frac{dS(t)}{dt} = \Lambda - \frac{\beta_e B(t)}{\kappa + B(t)} S(t) - \mu S(t), \tag{1}$$

$$\frac{dI(t)}{dt} = \frac{\beta_e B(t-\tau)e^{-\mu\tau}}{\kappa + B(t-\tau)} S(t-\tau) - (\mu + \delta + \gamma) I(t), \tag{2}$$

$$\frac{dR(t)}{dt} = \gamma I(t) - \mu R(t), \tag{3}$$

$$\frac{dB(t)}{dt} = \xi I(t) - (\eta - \nu) B(t). \tag{4}$$

The model equations (1)–(4) satisfy the nonnegative initial data

$$S(\theta) = \phi_1(\theta),\ I(\theta) = \phi_2(\theta),\ R(\theta) = \phi_3(\theta),\ B(\theta) = \phi_4(\theta),\ \theta \in [-\tau, 0], \tag{5}$$

where $\phi = (\phi_1, \phi_2, \phi_3, \phi_4) \in \mathcal{C}([-\tau, 0], \mathbb{R}^4_+)$, the space of continuous functions mapping $[-\tau, 0]$ into $\mathbb{R}^4_+$, equipped with the maximum norm (6), defined by

$$\| \phi \| = \max_{-\tau \le \theta \le 0} | \phi(\theta) |. \tag{6}$$

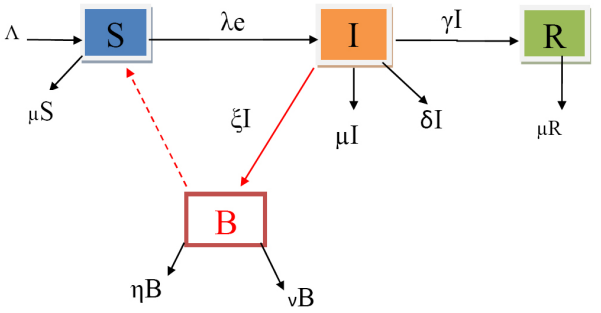


Figure 1

Schematic representation of the Cholera model (1)–(4).

3. Preliminary results

In this section, we present some preliminary results for the delay model (1)–(4) such as existence and uniqueness, positivity, boundedness of solution and calculation of basic reproduction number.

Theorem 1 : *The solution* $(S(t), I(t), R(t), B(t))$ *of the model* (1)–(4), *with initial data* (5) *exists, is unique and positive for all time* $t \geq 0$. *Moreover, the solution is bounded.*

Proof : We start with existence and uniqueness of the solution $(S(t), I(t), R(t), B(t))$. Let $X(t) = (S(t), I(t), R(t), B(t))$. The system (1)–(4), can be written as

$$\frac{dX}{dt} = f(t, X_t), \tag{7}$$

where $X_t(\theta) = X(t + \theta)$, for $\theta \in [-\tau, 0]$, f is Lipschitzian in X. It follows from Theorems 2.1 and 2.3 in [14] that the system (1)–(4) as represented in (7) has a unique solution $(S(t), I(t), R(t), B(t))$ satisfying the initial data (5).

Next, we consider the positivity of solution $(S(t), I(t), R(t), B(t))$. Assuming the initial condition in (5) holds, we prove that $S(t) > 0$, $I(t) > 0$, $R(t) > 0$, $B(t) > 0$ for all time $t \in (0, \infty)$.

Consider equation (1), we have

$$\frac{dS}{dt} \geq -\left[\frac{\beta_e B(t)}{\kappa + B(t)} + \mu\right] S(t), \text{ so that}$$

$$S(t) \geq S(0)\exp\left[-\int_0^t\left(\frac{\beta_e B(t)}{\kappa + B(t)} + \mu\right)du\right]$$
$$> 0.$$

Hence $S(t)$ is positive for any $t \in (0, \infty)$.

We now apply the contradiction approach by assuming that the other variables are non-positive. This will implies that there is a time $\hat{t} > 0$ such that $I(\hat{t}) = 0,\ B(\hat{t}) = 0,\ R(\hat{t}) = 0$ and $S(t) > 0$, $I(t) > 0$, $B(t) > 0$, $R(t) > 0$ for all $t \in [0, \hat{t})$ and $\frac{dI(\hat{t})}{dt} \leq 0$, $\frac{dB(\hat{t})}{dt} \leq 0$, $\frac{dR(\hat{t})}{dt} \leq 0$. Then it follows from (2),

$$\frac{dI(\hat{t})}{dt} = \frac{\beta_e B(\hat{t}-\tau)e^{-\mu\tau}}{\kappa + B(\hat{t}-\tau)}S(\hat{t}-\tau) > 0,$$

which contradicts our earlier assumption. Therefore, there is no such $\hat{t}$, hence $I(t)$ is positive $\forall\ t > 0$.

Similarly, from (4) we have,

$$\frac{dB(\hat{t})}{dt} = \xi I(\hat{t}) > 0,$$

which also contradicts our earlier assumption. Hence there is no such time $\hat{t}$, which implies that $B(t)$ is positive $\forall\ t > 0$.

Similar approach can be used to show that $R(t)$ is positive $\forall\ t > 0$. This proved the first part of Theorem 1.

To prove the boundedness of solution, we follow the approach in Lin *et al.* and Wang *et al.* [24, 43] by defining the function

$$V(t) \quad = S(t) + e^{\mu\tau} I(t + \tau). \tag{8}$$

Calculating the derivative of (8) with respect to t and from (1), (2), we obtain

$$\begin{aligned} V'(t) &= \Lambda - \frac{\beta_e B(t)}{\kappa + B(t)}S(t) - \mu S(t) + e^{\mu\tau}\left[\frac{\beta_e B(t)e^{-\mu\tau}}{\kappa + B(t)}S(t) - (\mu + \delta + \gamma)I(t+\tau)\right] \\ &= \Lambda - \mu S(t) - e^{\mu\tau}(\mu + \delta + \gamma)I(t+\tau), \\ &\leq \Lambda - \min\{\mu, (\mu + \delta + \gamma)\}V(t), \\ &\leq \Lambda - \mu V(t). \end{aligned}$$

so that

$$\limsup_{t\to\infty}[S(t) + e^{\mu\tau} I(t+\tau)] \leq \frac{\Lambda}{\mu}.$$

From (3), it follows that

$$\frac{dR(t)}{dt} \leq \frac{\Lambda\gamma e^{-\mu\tau}}{\mu} - \mu R(t),$$

hence,

$$\limsup_{t\to\infty} R(t) \leq \frac{\Lambda\gamma e^{-\mu\tau}}{\mu^2}.$$

Similarly, from (4), we have

$$\frac{dB(t)}{dt} \leq \frac{\Lambda\xi e^{-\mu\tau}}{\mu} - (\eta+\nu)B(t),$$

which implies that,

$$\limsup_{t\to\infty} B(t) \leq \frac{\Lambda\xi e^{-\mu\tau}}{\mu(\eta+\nu)}.$$

Therefore, the following set is positively invariant set for system (1) – (4):

$$\Omega = \left\{(S,I,R,B) : S + e^{\mu\tau} I \leq \frac{\Lambda}{\mu},\ R \leq \frac{\Lambda\gamma e^{-\mu\tau}}{\mu^2},\ B \leq \frac{\Lambda\xi e^{-\mu\tau}}{\mu(\eta+\nu)}\right\}. \tag{9}$$

That means any solution initiating in (9) or nearby, for all future time, the solution will be attracted and remains inside Ω. Thus, the solution ($S(t)$, $I(t)$, $R(t)$, $B(t)$) is ultimately bounded by a positive constant. This completes the proof. □

2. Equilibria and Control reproduction number

In this section, the existence of equilibria and their asymptotic stabilities will be discussed. Further- more, the computation of control reproduction number of the model will be shown. Linearizing model equations (1) - (4) about an arbitrary equilibrium and denoting

$$k_1 = (\mu + \delta + \gamma),\ k_2 = (\eta + \nu), \tag{10}$$

we get

$$\begin{bmatrix} \frac{dS(t)}{dt} \\ \frac{dI(t)}{dt} \\ \frac{dR(t)}{dt} \\ \frac{dB(t)}{dt} \end{bmatrix} = \begin{bmatrix} -\frac{\beta_e B}{\kappa+B} - \mu & 0 & 0 & -\frac{\kappa\beta_e S}{(\kappa+B)^2} \\ 0 & -k_1 & 0 & 0 \\ 0 & \gamma & -\mu & 0 \\ 0 & \xi & 0 & -k_2 \end{bmatrix} \begin{bmatrix} S(t) \\ I(t) \\ R(t) \\ B(t) \end{bmatrix} + \begin{bmatrix} 0 & 0 & 0 & 0 \\ \frac{\beta_e B e^{-\mu\tau}}{\kappa+B} & 0 & 0 & \frac{\kappa\beta_e S e^{-\mu\tau}}{(\kappa+B)^2} \\ 0 & 0 & 0 & 0 \\ 0 & 0 & 0 & 0 \end{bmatrix} \begin{bmatrix} S(t-\tau) \\ I(t-\tau \\ R(t-\tau) \\ B(t-\tau) \end{bmatrix} \tag{11}$$

4.1 *Equilibria of the model*

Equilibria of the model are obtained when the right sides of (1)–(4) are equated to zero. Further, at equilibrium, we have $S(t) = S(t-\tau) = S^*$, $I(t) = I(t-\tau) = I^*$, and $B(t) = B(t-\tau) = B^*$. Since $R(t)$ is not obtained in other equations, we decouple (3) so that we get

$$\Lambda - \left(\frac{\beta_e B^*}{\kappa + B^*}\right) S^* - \mu S^* = 0, \tag{12}$$

$$\left(\frac{\beta_e B^* e^{-\mu\tau}}{k + B^*}\right) S^* - k_1 I^* = 0, \tag{13}$$

$$\xi I^* - k_2 B^* = 0. \tag{14}$$

From (14), we let $k_3 = \frac{\xi}{k_2}$, so that

$$B^* = k_3 I^*. \tag{15}$$

Substituting the value of B^* above into (13), we have

$$I^*\left(\frac{\beta_e k_3 e^{-\mu\tau} S^*}{k + k_3 I^*} - k_1\right) = 0. \tag{16}$$

The case when $I^* = 0$ give rise to a unique disease-free equilibrium (DFE),

$$\mathcal{E}_0 = (S^0, I^0, B^0) = \left(\frac{\Lambda}{\mu}, 0, 0\right). \tag{17}$$

However, when $I^* \neq 0$, solving S^* from (16) gives

$$S^* = \frac{(k + k_3 I^*)k_1}{\beta_e k_3 e^{-\mu\tau}}. \tag{18}$$

Now substituting (15) and (18) in (12), we obtained the endemic equilibrium of the model as

$$\mathcal{E}^* = (S^*,\ I^*,\ B^*) = \left(\frac{(k + k_3 I^*)}{\beta_e k_3 e^{-\mu\tau}}, I^*,\ k_3 I^* \right), \tag{19}$$

where I^*, is the positive root for the second order polynomial

$$f(I^*) = (-\beta_e k_1 k_3^2 - \mu k_1 k_3^2)(I^*)^2 + (\Lambda \beta_e k_3^2 e^{-\mu\tau} - \beta_e k_1 k_3 \kappa - 2\mu k_1 k_3 \kappa) I^* + (\Lambda \beta_e k_3 \kappa e^{-\mu\tau} - \mu k_1 k^2) = 0. \tag{20}$$

We define $\mathcal{R} = \sqrt{\frac{\beta_e \xi \Lambda e^{-\mu\tau}}{\kappa \mu k_1 k_2}}$. Simplifying equation (20) further, we get

$$f(I^*) = A(I^*)^2 + BI^* + C = 0, \tag{21}$$

where

$$A = (-\beta_e k_1 k_3^2 - \mu k_1 k_3^2),\ B = [\mu k_1 k_3 \kappa (\mathcal{R}^2 - 1) - \beta_e k_1 k_3 \kappa - \mu k_1 k_3 \kappa],$$
$$C = \mu k_1 \kappa^2 (\mathcal{R}^2 - 1).$$

From equation (21), the two roots, I_1^* and I_2^* must satisfy

$$I_1^* I_2^* = \frac{C}{A} \text{ and } I_1^* + I_2^* = -\frac{B}{A}.$$

From the expressions of A, C, we have $A < 0$, $C > 0$ if $\mathcal{R} > 1$, and $I_1^* I_2^* = \frac{C}{A} < 0$. Thus, from (21), using Descartes Rule, $f(I^*)$ has one unique positive root $\left(I_1^* = \frac{-B + \sqrt{B^2 - 4AC}}{2B} \right)$, and sub-sequently, the endemic equilibrium (19) is uniquely determined. When $\mathcal{R} < 1$, all coefficients of $f(I^*)$ are negative, hence the roots of (20) are biologically nonfeasible (negative roots).

4.2 *Computation of control reproduction number ($\mathcal{R}_c$).*

According to [41], the control reproduction number $\mathcal{R}_c$ is defined as the average number of secondary cases produced by one infected individual introduced into a population of susceptible individuals in the presence of intervention. However, when there are control strategies, it is called control reproduction number. Following the method in [45, 50], we derive the control reproduction number, denoted by $\mathcal{R}_c$.

We define the "diseased compartments" as the infected humans (I) and concentration of the *V. cholerae* in aquatic reservoir (B). Linearizing (2) and (3) about $I(t)$, $I(t - \tau)$, $B(t)$ and $B(t - \tau)$, evaluating at DFE, we have

$$\frac{dI(t)}{dt} = \frac{\beta_e \Lambda e^{-\mu\tau}}{\kappa\mu} B(t-\tau) - k_1 I(t), \tag{22}$$

$$\frac{dB(t)}{dt} = -k_2 B(t) + \xi I(t). \tag{23}$$

Let $y_1(0)$ and $y_2(0)$ be the number of infectious humans and concentration of cholera introduced at $t = 0$. Then the remaining infectious humans and cholera concentration at time $t > 0$, are given by

$$y_1(t) = y_1(0)e^{-k}1t, \tag{24}$$

$$y_2(t) = y_2(0)e^{-k}2t. \tag{25}$$

Thus, the total numbers of newly infected humans and concentration of cholera are

$$\overline{y}_1 = \int_\tau^\infty \frac{\beta_e \Lambda e^{-\mu\tau}}{\kappa\mu} y_2(0) e^{-k_2(t-\tau)} dt, \tag{26}$$

$$\overline{y}_2 = \int_0^\infty \xi y_1(0) e^{-k_1 t} dt \tag{27}$$

Hence,

$$\overline{y}_1 = \frac{\beta_e \Lambda e^{-\mu\tau}}{\kappa\mu k_2} y_2(0), \tag{28}$$

$$\overline{y}_2 = \frac{\xi}{k_1} y_1(0). \tag{29}$$

Equations (28)–(29) can be expressed in matrix form as

$$\begin{bmatrix} \overline{y}_1 \\ \overline{y}_2 \end{bmatrix} = \begin{bmatrix} 0 & \dfrac{\beta_e \Lambda e^{-\mu\tau}}{\kappa\mu k_2} \\ \dfrac{\xi}{k_1} & 0 \end{bmatrix} \begin{bmatrix} y_1(0) \\ y_2(0) \end{bmatrix}.$$

The matrix $\mathcal{M}_0 = \begin{bmatrix} 0 & \dfrac{\beta_e \Lambda e^{-\mu\tau}}{\kappa\mu k_2} \\ \dfrac{\xi}{k_1} & 0 \end{bmatrix}$, is the next infection operator.

We define the spectral radius of $\mathcal{M}_0$ as the control reproduction number for the model. Thus

$$\mathcal{R}_c = \rho(\mathcal{M}_0) = \sqrt{\frac{\beta_e \xi \Lambda e^{-\mu\tau}}{\kappa\mu k_1 k_2}}. \tag{30}$$

It can be noticed that the control reproduction number $\mathcal{R}_c = \mathcal{R}$.

4.3 *Stability of the disease-free equilibrium*

In this subsection, the local and global stability results of disease-free equilibrium, E_0, are presented.

Theorem 2 : *The disease-free equilibrium* $\mathcal{E}_0 = \left(\frac{\Lambda}{\mu}, 0, 0\right)$ *is locally asymptotically stable if* $\mathcal{R}_c < 1$ *and unstable when* $\mathcal{R}_c > 1$. *Furthermore,* $\mathcal{E}_0$ *is globally asymptotically stable if* $\mathcal{R}_c < 1$.

Proof : Assuming a solution of the form $X(t) = e^{\lambda t}$, where $X(t) = (S(t), I(t), B(t))$ and λ is an eigenvalue. The transcendental equation of system (11), evaluated at $\mathcal{E}_0$, assuming nontrivial solution, is

$$G(\lambda) = (\lambda + \mu)\left[(\lambda + k_1)(\lambda + k_2) - \frac{\beta_2 \xi \Lambda e^{-\tau(\lambda+\mu)}}{\kappa\mu}\right]. \tag{31}$$

Obviously, one of the eigenvalues in (31), $\lambda_1 = -\mu$ is negative. Hence the stability of $\mathcal{E}_0$ is determined by the signs of the remaining eigenvalues in (31) defined as

$$g_1(\lambda) = \lambda^2 + [\mathrm{k}_1 + \mathrm{k}_2]\lambda + k_1 k_2 - \frac{\beta_e \xi e^{-t(\lambda+\mu)}\Lambda}{\kappa\ \mu}. \tag{32}$$

From (32) we have

$$g_1(0) = \mathrm{k}_1\, k_2(1 - \mathcal{R}_c^2).$$

If $\mathcal{R}_c > 1$, then $g_1(0) < 0$. Since $g_1(\lambda)$ goes to ∞ as λ approaches ∞, $g_1(\lambda)$ has at least one eigenvalue with positive root, hence $\mathcal{E}_0$ is unstable. However, when $\mathcal{R}_c < 1$, then there is no root with positive real part that can satisfy $g_1(\lambda)$.

Furthermore, to verify the existence of Hopf bifurcation, we assume that $\lambda = iy$ with $y \in \mathbb{R}_+$ be a root of $g_1(\lambda) = 0$. From (32), we have

$$g_1(iy) = -y^2 + [k_1 + k_2]iy + k_1 k_2 - \frac{\beta_e \xi e^{-\tau\mu}\Lambda}{\kappa\ \mu}(\cos\tau y - i\sin\tau y) = 0.$$

Thus, equating real and imaginary parts:

$$-y^2 + k_1 k_2 = \frac{\beta_e \xi e^{-\tau\mu}\Lambda}{\kappa\ \mu}\cos\tau y,$$

$$[k_1 + k_2]y = -\frac{\beta_e \xi e^{-\tau\mu}\Lambda}{\kappa\,\mu}\sin\tau y.$$

Squaring both sides and adding the two equations, we obtain

$$y^4 + (k_1^2 + k_2^2)y^2 + k_1^2k_2^2 - \left(\frac{\beta_e \xi e^{-\tau\mu}\Lambda}{\kappa\,\mu}\right)^2 = 0. \tag{33}$$

Let $\omega = y^2$, then from equation (33),

$$\omega^2 + [k_1^2 + k_2^2]\omega + k_1^2k_2^2 - \left(\frac{\beta_e \xi e^{-\tau\mu}\Lambda}{\mu}\right)^2 = 0. \tag{34}$$

The necessary condition for (34), to have no positive roots is for $k_1^2k_2^2 - \left(\frac{\beta_e \xi e^{-\tau\mu}\Lambda}{\kappa\,\mu}\right)^2 > 0$. Now,

$$k_1^2k_2^2 - \left[\frac{\beta_e \xi e^{-\tau\mu}\Lambda}{\kappa\,\mu}\right]^2 = k_1^2k_2^2\left[1 - \left(\frac{\beta_e \xi e^{-\tau\mu}\Lambda}{\kappa\,\mu k_1 k_2}\right)^2\right],$$
$$= k_1^2k_2^2(1 - \mathcal{R}_c),$$

If $\mathcal{R}_c > 1$, then $g_1(\lambda)$ has at least one positive root and therefore, the DFE, $\mathcal{E}_0$ is unstable. However, if $\mathcal{R}_c < 1$, then $g_1(\lambda)$ has no positive roots and, the *DFE* $\mathcal{E}_0$, is locally asymptotically stable for all values of the delay $\tau \geq 0$. This proves the first part of the Theorem.

Finally, to complete the proof of Theorem 2, we need to show the global attractiveness of $\mathcal{E}_0$ when $\mathcal{R}_c < 1$. This will be explored using the approach used in [25] as follows.

From the linearized form of (22)–(23), we get

$$\frac{dI(t)}{dt} = \frac{\beta_e \Lambda e^{-\mu\tau}}{\kappa\,\mu}B(t-\tau) - k_1 I(t),$$
$$\frac{dB(t)}{dt} = -k_2 B(t) + \xi I(t).$$

Let the following linear system be given:

$$\frac{dx_1(t)}{dt} = \left(\frac{\beta_e \Lambda e^{-\mu\tau}}{\kappa\,\mu}\right)x_2(t-\tau) - k_1 x_1(t), \tag{35}$$

$$\frac{dx_2(t)}{dt} = -(\eta + \nu)x_2(t) + \xi x_1(t). \tag{36}$$

The system (35) – (36) represent a competitive and irreducible system of delay differential equations with a unique equilibrium $(B^*, I^*) = (0, 0)$ [25].

Hence

$$\lim_{t\to\infty}(x_1(t),\ x_2(t)) = (0,\ 0).$$

Using the standard comparison argument we have

$$\lim_{t\to\infty}(I(t),\ B(t)) = (0,\ 0).$$

Therefore from (1)–(4), we have the following limiting system

$$\frac{dS(t)}{dt} = \Lambda - \mu S(t),$$

so that

$$\lim_{t\to\infty}(S(t), I(t), B(t)) = \left(\frac{\Lambda}{\mu}, 0, 0\right).$$

Using the theory of asymptotically autonomous systems [39], the *DFE* $\mathcal{E}_0$, is globally asymptotically stable for all values of the delay $\tau \geq 0$ when $\mathcal{R}_c < 1$. □

4.4 *Stability of endemic equilibrium*

In this part, the local stability result for, $\mathcal{E}^* = (S^*, I^*, B^*)$, given in (19) and possible occurrence of Hopf bifurcation will be explored with delay τ as the parameter. From (11), the transcendental equation evaluated at $\mathcal{E}^*$ is given by

$$H(\lambda) = \lambda^3 + P_2\lambda^2 + P_1\lambda + P_0 + (Q_1\lambda + Q_0)e^{-\tau(\lambda+\mu)}, \tag{37}$$

where

$$P_2 = \left(k_1 + k_2 + \mu + \frac{\beta_e B^*}{\kappa + B^*}\right),$$

$$P_1 = (k_1 + k_2)\left(\frac{\beta_e B^*}{\kappa + B^*} + \mu\right) + k_1 k_2,$$

$$P_0 = k_1 k_2 \mu + \frac{k_1 k_2 \beta_e B^*}{\kappa + B^*},$$

$$Q_1 = -\frac{\kappa \xi \beta_e S^*}{(\kappa + B^*)}, \text{ and } Q_0 = \frac{\mu \kappa \xi \beta_e S^*}{(\kappa + B^*)^2}. \tag{38}$$

To study the local stability behavior, we need to established that the real parts of all the eigenvalues of transcendental equation (37) are negative or there is at least one positive root of which the stability will be conditional on τ. For the later, we explore the conditions for Hopf-bifurcation of $\mathcal{E}^*$ with delay τ as a parameter. First, the stability of equation (37) has to be determined when $\tau = 0$.

If $\tau = 0$, equation (37) becomes

$$H(\lambda) = \lambda^3 + P_2\lambda^2 + P_1\lambda + P_0 + (Q_1\lambda + Q_0). \tag{39}$$

Here, we need to show that all the solutions of (39) are negative. When $\lambda = 0$, from equations (19), (38) and (39), we have

$$\begin{aligned} H(0) &= k_1 k_2 \mu - \frac{\kappa \xi \beta_e \mu S^* e^{-\mu\tau}}{(\kappa + B^*)^2} + \frac{k_1 k_2 \beta_e B^*}{\kappa + B^*}, \\ &= k_1 k_2 \mu - \frac{\kappa k_1 k_2 \mu}{\kappa + B^*} + \frac{k_1 k_2 \beta_e B^*}{\kappa + B^*} \\ &= k_1 k_2 \mu \left[1 - \frac{\kappa}{\kappa + B^*} \right] + \frac{k_1 k_2 \beta_e B^*}{\kappa + B^*} > 0, \end{aligned}$$

and $\lim_{\lambda \to \infty} H(\lambda) = +\infty.$

Hence, $H(\lambda) = 0$ has no positive root in $[0, +\infty)$. Thus, all the roots of $H(\lambda) = 0$ have negative real parts, therefore $\mathcal{E}^*$ is locally asymptotically stable when $\tau = 0$.

Furthermore, when $\tau > 0$, to rule out the possibility of complex conjugate roots, assume there is a root $\lambda = i\omega$ of (37), with $\omega \in \mathbb{R}^+$, where the positive root will cross the imaginary axis. Thus, putting $\lambda = i\omega$ in (37) and simplifying by considering real and imaginary parts, we have

$$-P_2\omega^2 + P_0 = -Q_1\omega e^{-\mu\tau} \sin \omega\tau - Q_0 e^{-\mu\tau} \cos \omega\tau, \tag{40}$$

$$-\omega^3 + P_1\omega = -Q_1 e^{-\mu\tau}\, \omega \cos \omega\tau + Q_0 e^{-\mu\tau} \sin \omega\tau. \tag{41}$$

By Squaring and summing (40) and (41), we get

$$\omega^6 + (P_2^2 - 2P_1)\omega^4 + (P_1^2 - 2P_2P_0 - Q_1^2 e^{-2\mu\tau})\omega^2 + P^2 - Q_0^2 e^{-2\mu\tau} = 0. \tag{42}$$

Letting $\omega^2 = y$, equation (42) can be rewritten as

$$F(y) = y^3 + B_2y^2 + B_1y + B_0 = 0, \tag{43}$$

where $B_2 = P_2^2 - 2P_1$, $B_1 = (P_1^2 - 2P_2P_0 - Q^2e^{-2\mu\tau})$, and $B_0 = P_0^2 - Q_0^2e^{-2\mu\tau}$.

Differentiating equation (43) with respect to y, we get

$$F'(y) = 3y^2 + 2B_2y + B_1. \tag{44}$$

Noting that the roots of $F'(y)$ are

$$y_1 = \frac{-B_2 + \sqrt{B_2^2 - 3B_1}}{3} \text{ and } y_2 = \frac{-B_2 - \sqrt{B_2^2 - 3B_1}}{3}. \tag{45}$$

Following the approach in [21], let $\Delta = B_2^2 - 3B_1$, then we have the following possibilities

(i) If $\Delta \le 0$, then $F'(y) \ge 0$. Thus $F(y)$ is monotone increasing. Therefore when $B_0 = F(0) \ge 0$ and $\Delta \le 0$, equation (43) has no positive roots, and all eigenvalues of (37) will have negative real parts for all $\tau > 0$.

(ii) If $B_0 < 0$, since $\lim_{y\to\infty} F(y) = +\infty$, equation (43) has one or more at positive root, and eigenvalues can jump to the right half plane through the imaginary axis.

(iii) If $\Delta > 0$, then the graph of $F(y) = 0$ has turning points at $y_1^c = \frac{-B_2 + \sqrt{\Delta}}{3}$ and $y_2^c = \frac{-B_2 - \sqrt{\Delta}}{3}$. If $y_1{}^c > 0$ and $F(y_1{}^c) < 0$, then $F(y) = 0$ has positive roots.

Remark 4.1 : Conditions (i) - (iii) Give possibilities for occurrence of Hopf bifurcation or otherwise with regards to the stability of $\mathcal{E}^*$. However, there is need to stress that if in particular, condition (ii) is satisfied, then the stability of $\mathcal{E}^*$ is conditioned on the delay value.

Suppose condition (ii) is satisfied, then without loss of generality, let the roots of $F(y) = 0$ be y_1, y_2, y_3, so that $\omega_i = \sqrt{y_j}$, for $1 \le j \le 3$.

Solving equations (40) - (41), we get the expression for τ, as

$$\tau_i = \frac{1}{\omega_i}\arctan\left[\frac{(P_2Q_1 - Q_0)\omega_i^3 + (P_1Q_0 - P_0Q_1)\omega_i}{-Q_1\omega_i^4 + (P_1Q_1 - P_2Q_0)\omega_i^2 + P_0Q_0}\right] \tag{46}$$

Let

$$\tau_0 = \tau_c = \min_{1\le i\le 3}\{t_i \mid y_i \text{ is a positive root of F(y)} = 0\},$$

$$\omega_0 = \omega_i. \tag{47}$$

Hence, τ_c is the first critical delay where the eigenvalues will traverse the imaginary axis at $\pm i\omega_0$.

Thus, the stability results of $\mathcal{E}^*$ can be summarized and stated as follows.

Theorem 3 :

(1) *The endemic equilibrium $\mathcal{E}^*$, when $\mathcal{R}_c > 1$, is locally asymptotically stable for all delay $\tau > 0$ if $B_0 \geq 0$ and $\Delta \leq 0$.*

(2) *If either (a) $B_0 < 0$, or (b) $\Delta > 0$, $y_1^c = \frac{-B_2+\sqrt{\Delta}}{3} > 0$ and $F(y_1^c) < 0$, then there exists a critical delay τ_0 and ω_0 as defined in* (47)*, such that $\mathcal{E}^*$ is locally asymptotically stable for $\tau \in [0, \tau_0)$. In addition, if $F'(\omega_0) \neq 0$, then the model exhibit Hopf bifurcation at $\mathcal{E}^*$ with $\tau = \tau_0$.*

Proof : The proof of Theorem 3 is given above, it now remains to show the transversality condition for the existence of Hopf bifurcation at $\tau = \tau_0$.

Differentiating equation (37) in τ, we have

$$\left[\frac{d\lambda}{d\tau}\right]^{-1} = \frac{(3\lambda^2 + 2P_2\lambda + P_1)e^{\tau(\eta\lambda)}}{\lambda(Q_1\lambda + Q_0)} + \frac{Q_1}{\lambda(Q_1\lambda + Q_0)} - \frac{\tau}{\lambda}, \tag{48}$$

Hence, using equations (40) and (41),

$$\begin{aligned}
\left[\frac{d(\mathrm{Re}(\lambda))}{d\tau}\right]^{-1}_{\tau=\tau_0} &= \mathrm{Re}\left[\frac{(3\lambda^2 + 2P_2\lambda + P_1)e^{\tau(\eta\lambda)}}{\lambda(Q_1\lambda + Q_0)}\right] + \mathrm{Re}\left[\frac{Q_1}{\lambda(Q_1\lambda + Q_0)}\right] \\
&= \frac{1}{Q_1^2\omega^4 + Q_0^2\omega_0^2}\{e^{\tau_0\eta}[2P_2\omega_0(Q_0\sin\omega_0\tau_0 - Q_1\omega_0\cos\omega_0\tau_0]\} \\
&\quad -P_1(Q_0\cos\omega_0\tau_0 + Q_1\sin\omega_0\tau_0)] - Q_1Q_0\}, \\
&= \frac{(3\omega_0^6 + 2B_2\omega_0^4 + B_1w_0^2)e^{\tau_0\eta}}{Q_1^2\omega_0^4 + Q_0^2\omega_0^2}, \\
&= \frac{F'(\omega_0^2)}{Q_1^2\omega_0^4 + Q_0^2\omega_0^2}.
\end{aligned} \tag{49}$$

Hence from (49)

$$sign\left[\frac{d(\mathrm{Re}(\lambda))}{d\tau}\right]^{-1}_{\tau=\tau_0} = sign\,F'(\omega_0^2). \tag{50}$$

Therefore, if $F'(\omega_0^2) \neq 0$, the transversality condition holds [19, 26, 33] and a Hopf bifurcation occurs at $\tau = \tau_0$. At this point, family of solutions will bifurcate from $\mathcal{E}^*$. This completes the proof. □

5. Numerical simulations

Table 1

Description of Parameter values with references for the model

Parameter	Description	Value	Range	Reference
β_e	Contamination rate	0.2143 day^{-1}	0.0001 – 17.73	[18, 22, 34, 44]
κ	Concentration of *V. cholerae* in the environment	10^6 cellsml^{-1}	500 – 10^{10}	[6, 27, 31, 38]
η	Decay rate of cholera	0.33 day^{-1}	0.023 – 1.06	[6, 11, 22, 31]
ν	Disinfection rate	$\frac{4}{365} day^{-1}$	$\frac{4}{365} - \frac{100}{365}$	[38]
Λ	Recruitment rate of humans	15 day^{-1}	4 – 10^4	[17, 18, 32, 53]
μ	Human natural death rate	0.000442 day^{-1}	0.000038 – 0.000442	[15, 23, 27, 38]
γ	Recovery rate	0.10025 day^{-1}	0.0005 – 0.2	[11, 22, 31]
Δ	Cholera induced death rate	0.015 day^{-1}	0.0000627 – 0.015	[23, 38, 51, 52]
ξ	Shedding rate of *V. cholarae* by infected humans	4 day^{-1}	1 – 120	[6, 18, 22, 27]

In Figure 2, the global asymptotic stability of disease-free equilibrium $\mathcal{E}_0$, is shown using parameter values from Table 1, various initial values with small delay $\tau = 2$ and $\beta_e = 0.343$ giving the value of $\mathcal{R}_c = 0.819 < 1$. It can be seen that the numbers of susceptible humans Figure 2(a), infected humans Figure 2(b), concentration of cholera Figure 2(c) and phase portrait of these populations Figure 2(d), using unequal initial functions, approach the equilibrium $\mathcal{E}_0$. This illustrates the result in Theorem 2. To illustrate the result in Theorem 2 further, Figures 3(a)-(d) are obtained using the same param- eters as in Figure 2, except for the delay value $\tau = 60$ and $\beta_e = 7.343$,

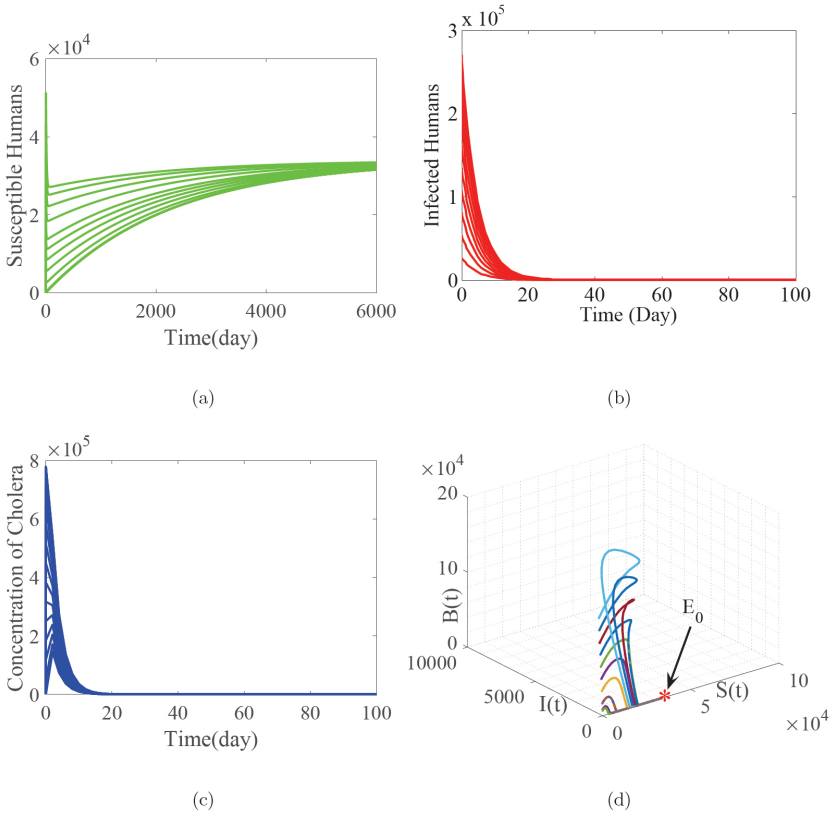


Figure 2

Numerical simulations depicting the global stability of disease free equilibrium $\mathcal{E}_0$ with parameter values in Table 1 and different initial values, except for $\tau = 2$, $\beta_e = 0.343$, so that $\mathcal{R}_c = 0.8191 < 1$. In (a) susceptible humans, (b) infected humans, (c) concentration of cholera in the environment and (d) phase portrait of *S*, *I*, *B*.

so that $R_c = 0.3281 < 1$. The Figures 2(a) - 3(d) indicates that the disease-free equilibrium E_0, is LAS for any value of delay τ when $\mathcal{R}_c < 1$.

Figures 4(a)-(d) depict the local asymptotic stability of endemic equilibrium $\mathcal{E}^*$ using the parameter values in Table 1 with short delay $\tau = 3$, $\Lambda = 100$, $\xi = 50$, $\beta_e = 0.143$ which give $\mathcal{R}_c = 7.517 > 1$.

It can be seen that the number of (a) susceptible humans, (b) infected humans, (c) concentration of cholera and the two populations move to $\mathcal{E}^*$, when $\mathcal{R}_c > 1$. These figures, elucidate the result of Theorem 3.

Similarly, Figures 5(a)-(d) illustrates the local attractiveness for $\mathcal{E}^*$ using the parameter values in Table 1 with longer delay $\tau = 23$, $\Lambda = 150$, $\xi = 100$, $\beta_e = 17.73$ so that $\mathcal{R}_c = 4.792 > 1$. Here also, the populations move toward the endemic equilibrium $\mathcal{E}^*$ asymptotically.

The effect of time delay as the period between oral intake of contaminated water or food by susceptibles to full cholera infection in the population are shown in Figures 6(a)-(c). As can be seen in Figures 6(a) and 6(b), as the delay varies from $\tau = 2$ to $\tau = 14$, the number of infected humans decrease. This implies that, if the delay is short, the susceptibles progress

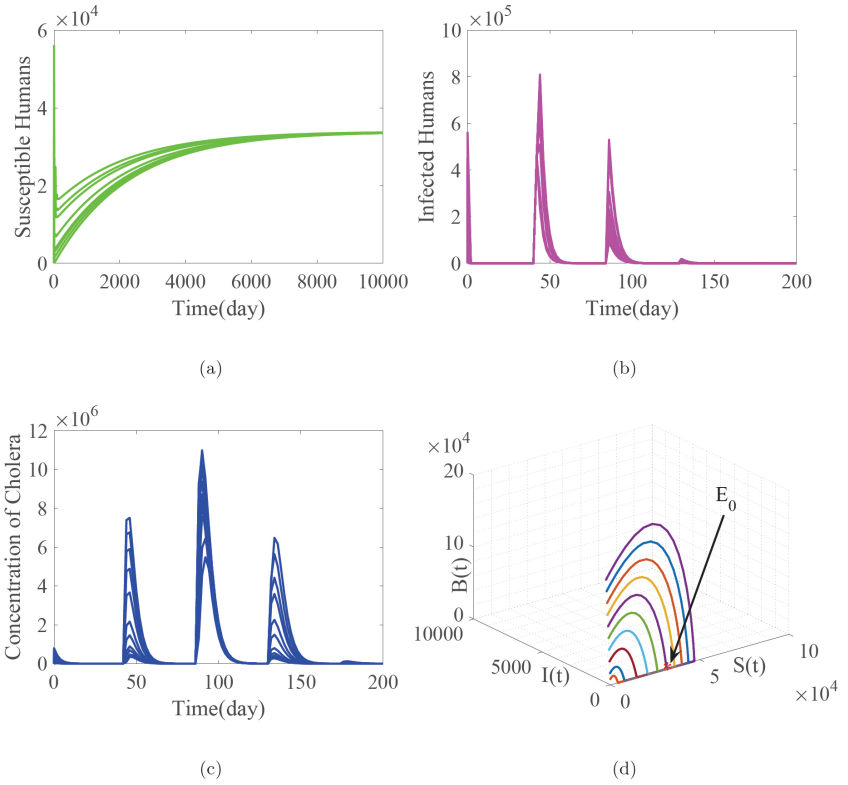


Figure 3

Numerical simulations illustrating global stability of disease-free equilibrium E_0 with parameter values in Table 1 and different initial values, except for $\tau = 60$, $\beta_e = 7.343$, so that $R_c = 0.3281 < 1$. In (a) susceptible humans, (b) infected humans, (c) concentration of cholera in the environment and (d) phase portrait of the populations.

fast to infectives, thus making the number of susceptibles less and more infectives. On the other hand, for longer time delay, susceptibles remain in their compartment for longer time, thus resulting in more susceptibles and less infectives. However, in Figure 6(c), as the delay is increased from $\tau = 2$ to $\tau = 14$, the concentration of cholera in the environment decreases. This has the same explanation as infective humans. Similarly, to study the effect of disinfection of environment as a control strategy, we simulate the model fixing all parameter values and varying the disinfection parameter, ν,

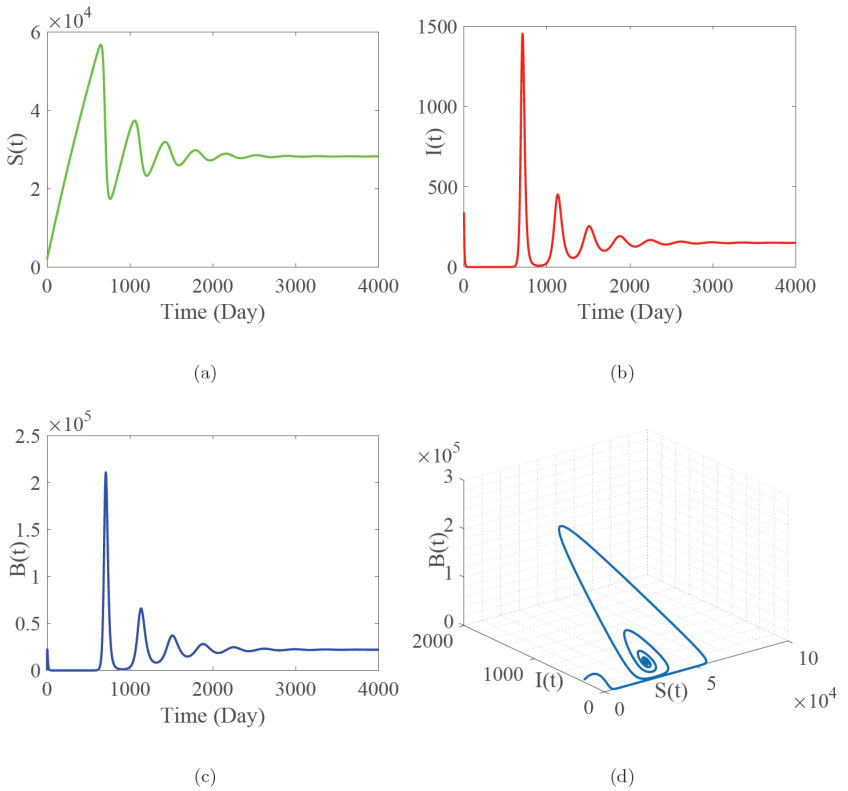


Figure 4

Time series for number of humans and concentration of cholera for the model (1)–(4) illustrating the local asymptotic stability of endemic equilibrium $\mathcal{E}^*$. Parameter values used as in Table 1, except for $\tau = 3$, $\Lambda = 100$, $\xi = 50$, $\beta_e = 0.143$ given $\mathcal{R}_c = 7.517 > 1$. In (a) susceptible humans, (b) infected humans, (c) concentration of cholera in the environment and (d) phase portrait of the populations.

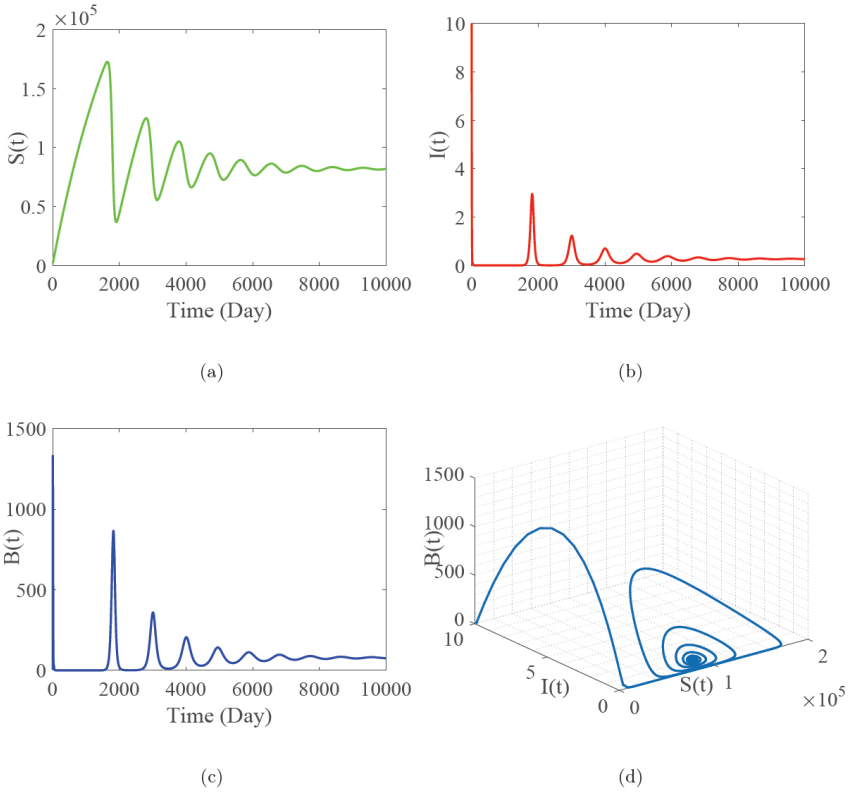


Figure 5

Numerical simulations for number of humans and concentration of cholera for the model (1)–(4) displaying the local asymptotic behaviour of $\mathcal{E}^*$ using longer delay. Parameter values used as in Table 1, except for $\tau = 23$, $\Lambda = 150$, $\xi = 100$, $\beta_e = 17.73$ given $\mathcal{R}_c = 4.792 > 1$. In (a) susceptible humans, (b) infected humans, (c) concentration of cholera in the environment and (d) phase portrait of the populations.

from $\frac{4}{365}$ to $\frac{100}{365}$ with $\tau = 5$. It can be seen from Figures 7(a) and (b) that the number of susceptible humans increase with increasing disinfection while the concentration of cholera decreases with increasing disinfection rate. The implication for this is that, since the infection comes from the environment only, disinfection effect will reduce the number of cholera pathogens and increase the susceptible humans invariably.

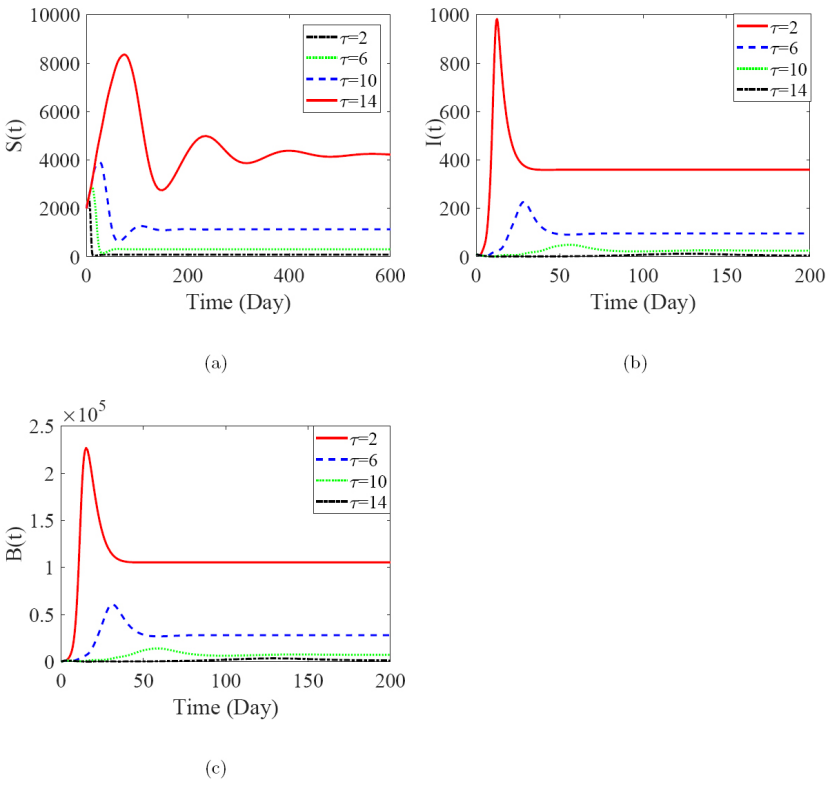


Figure 6

Numerical simulations of model (1)–(4) showing the effect of delay using the parameter values in Table 1, except for $\tau = 2$, 6, 10 and 14 in (a) susceptible humans, (b) infected humans and (c) concentration of cholera.

6. Conclusion

In this paper, a delay differential equation model for transmission of cholera in human population with infection from cholera in aquatic environment only is formulated and analyzed. The delay here represents the period between oral intake of contaminated water or food by susceptibles to full cholera infection in the population. Furthermore, a linear term for disinfection of cholera in the environment is incorporated as control strategy for the disease. We examine the basic properties of the model that guaranteed further study from both mathematical and biological perspectives. The major contributions in this paper can be summarized as follows:

(i) A unique cholera-free equilibrium for the model is determined and applied to systematically compute the control reproduction number $\mathcal{R}_c$; a threshold quantity for stability and disease control. Furthermore, this equilibrium is globally asymptotically stable for all delay value when $\mathcal{R}_c < 1$. Thus, cholera can be controlled if R_c is brought and maintained below unity. However, when $\mathcal{R}_c > 1$, the disease-free equilibrium is unstable, subsequently, a unique cholera endemic equilibrium emerges which is locally asymptotically stable for any delay value in its feasible region.

(ii) Critical delay value is determined and conditions for Hopf bifurcation are given.

(iii) In addition to the time delay being a threshold for stability, it is also shown to have influence in endemicity of the disease. For shorter delays, the numbers of healthy individuals is low while that of infected and concentration of cholera are high. However, for longer delays, the number of healthy individuals is high and that of infected and concentration of cholera gets lower drastically.

(iv) Varying the disinfection of cholera has revealed the increase/decrease the susceptibles population and concentration of cholera in a reciprocal manner.

(v) Numerical simulations are conducted to support all our results.

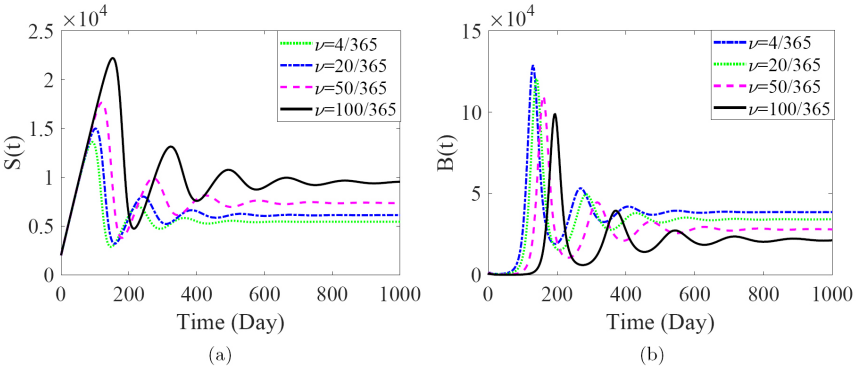


Figure 7

Numerical simulations for effect of disinfection of environment using parameter values in Table 1, except, for $\nu = \frac{4}{365}, \frac{20}{365}, \frac{50}{365}$ and $\frac{100}{365}$ in (a) susceptible humans, (b) concentration of cholera.

Acknowledgments

The authors are thankful to Pauline van den Driessche, University of Victoria, Canada and Daozhou Gao, Department of Mathematics, Shangai Normal University, Shangai, China for their valuable suggestions. A. S. Hassan acknowledges with thanks the support of Research Support Directorate, University of South Africa for the Research Grant Fellowship number 409000.

Disclosure statement

The authors hereby declare that there is no conflicts of interest whatsoever.

References

[1] J. F. T. Akoachere and C. K. Mbuntcha. Water sources as reservoirs of Vibrio cholerae O1 and non-O1 strains in Bepanda, Douala (Cameroon): Relationship between isolation and physico- chemical factors. *BMC Infectious Diseases*, 14(1):1–10, 2014.

[2] S. Almagro-Moreno and R. K. Taylor. Cholera: Environmental reservoirs and impact on disease transmission. *Microbiology Spectrum*, 1(2):1–19, 2013.

[3] S. Awasthi, N. Kumar, and P. K. Srivastava. An epidemic model to analyze the dynamics of malware propagation in rechargeable wireless sensor network. *Journal of Discrete Mathematical Sciences and Cryptography*, 24(5):1529–1543, 2021.

[4] E. Beretta and Y. Kuang. Modeling and analysis of a marine bacteriophage infection. *Mathe- matical Biosciences*, 149:57–76, 1998.

[5] V. Bhatnagar, R. C. Poonia, P. Nagar, V. Singh, L. Raja, and P. Dass. Descriptive analysis of COVID-19 patients in the context of India. *Journal of Interdisciplinary Mathematics*, 24(3):489– 504, 2021.

[6] L. M. Cai, C. Modnak, and J. Wang. An age-structured model for cholera control with vaccination. *Applied Mathematics and Computation*, 299:127–140, 2017.

[7] V. Capasso and S. L. Paveri-Fontana. A mathematical model for the 1973 cholera epidemic in the European Mediterranean region. *Rev. Epidemiol. Sante Publique*, 27(2):121–132, 1979.

[8] C. Chen, L. Liu, and N. Zhao. Fear Sentiment , Uncertainty , and Bitcoin Price Dynamics : The Case of COVID-19. *Emerging Markets Finance and Trade*, 56(10):2298–2309, 2020.

[9] C. T. Codeço. Endemic and epidemic dynamics of cholera: the role of the aquatic reservoir. *BMC Infectious Diseases*, 1(1):1–14, 2001.

[10] R. R. Colwell and A. Huq. Environmental reservoir of Vibrio cholerae the causative agent of cholera. *Annals of the New York Academy Society*, 740:44–54, 1994.

[11] E. Dangbé, D. Irépran, A. Perasso, and D. Békollé. Mathematical modelling and numerical simulations of the influence of hygiene and seasons on the spread of cholera. *Mathematical Biosciences*, 296(2018):60–70, 2017.

[12] ECDC. Communicable disease threats report, 17 -23 October 2021, week 42. Technical Report October, 2021.

[13] K. Gallandat, A. Huang, J. Rayner, G. String, and D. S. Lantagne. Household spraying in cholera outbreaks : Insights from three exploratory , mixed- methods field effectiveness evaluations. *PLoS Neglected Tropical Diseases*, 14(8):1–18, 2020.

[14] J. K. Hale and S.M.V. Lunel, Introduction to Functional Differential Equations, A*pplied Mathematical Sciences*, Springer-Verlag, New York Inc., 1993.

[15] D. M. Hartley, J. G. Morris, and D. L. Smith. Hyperinfectivity: A critical element in the ability of V. cholerae to cause epidemics? *PLoS Medicine*, 3(1):63–69, 2006.

[16] O. B. Hassan and L. B. Nellums. Cholera during COVID-19: The forgotten threat for forcibly displaced populations. *EClinicalMedicine*, 32:1–2, 2021.

[17] S. D. Hove-Musekwa, F. Nyabadza, C. Chiyaka, P. Das, A. Tripathi, and Z. Mukandavire. Mod- elling and analysis of the effects of malnutrition in the spread of cholera. *Mathematical and Computer Modelling*, 53:1583–1595, 2011.

[18] E. Kokomo and Y. Emvudu. Mathematical analysis and numerical simulation of an age-structured model of cholera with vaccination and demographic movements. *Nonlinear Analysis: Real World Applications*, 45:142–156, 2019.

[19] Y. Kuang. Delay Differential Equations with Applications in Population Dynamics. Academic Press, 1993.

[20] J. Li, Z. Teng, and L. Zhang. Stability and bifurcation in a vector-bias model of malaria trans- mission with delay. *Mathematics and Computers in Simulation*, 152:15–34, 2018.

[21] M. Y. Li and H. Shu. Global dynamics of a mathematical model for HTLV-I infection of CD4 + T cells with delayed CTL response. *Nonlinear Analysis: Real World Applications*, 13(3):1080–1092, 2012.

[22] S. Liao and F. Fang. Stability analysis and optimal control of a cholera model with time delay. *Journal of Computational Analysis and Applications*, 22(6):1055–1073, 2017.

[23] S. Liao and W. Yang. Cholera model incorporating media coverage with multiple delays. *Math- ematical Methods in the Applied Sciences*, 42(2):419–439, 2019.

[24] J. Lin, R. Xu, and X. Tian. Threshold dynamics of an HIV-1 virus model with both virus-to-cell and cell-to-cell transmissions, intracellular delay, and humoral immunity. *Applied Mathematics and Computation*, 315(11371368):516–530, 2017.

[25] J. Liu, L. Liu, X. Feng, and J. Feng. Global dynamics of a time-delayed echinococcosis transmis- sion model. *Advances in Difference Equations*, 2015(99), 2015.

[26] J. E. Marsden and M. McCracken. *The Hopf Bifurcation and Its Applications*. Springer-Verlag NewYork,, United States of America, 1976.

[27] A. K. Misra, A. Gupta, and E. Venturino. Cholera dynamics with Bacteriophage infection: A mathematical study. *Chaos, Solitons and Fractals*, 91:610–621, 2016.

[28] A. K. Misra, S. N. Mishra, A. L. Pathak, P. Misra, and R. Naresh. Modeling the effect of time delay in controlling the carrier dependent infectious disease - Cholera. *Applied Mathematics and Computation*, 218(23):11547–11557, 2012.

[29] A. K. Misra and V. Singh. A delay mathematical model for the spread and control of water borne diseases. *Journal of Theoretical Biology*, 301:49–56, 2012.

[30] Z. Mukandavire, S. Liao, J. Wang, H. Gaff, D. L. Smith, and J. G. Morris. Estimating the reproductive numbers for the 2008-2009 cholera outbreaks in Zimbabwe. *Proceedings of the National Academy of Sciences, USA*, 108(21):8767–8772, 2011.

[31] Z. Mukandavire, D. L. Smith, and J. G. Morris. Cholera in Haiti: Reproductive numbers and vaccination coverage estimates. *Scientific Reports*, 3:1–8, 2013.

[32] H. J. B. Njagarah. Modelling water-borne infections : the impact of hygiene, metapopulation movements and the biological control of cholera. PhD thesis, Stellenbosch University, 2014.

[33] G. Orosz. Hopf bifurcation calculations in delayed systems. *Journal of Nonlinear Science*, 14(6):505–528, 2004.

[34] D. Posny, C. Modnak, and J. Wang. A multigroup model for cholera dynamics and control. *International Journal of Biomathematics*, 9(1):27, 2016.

[35] M. A. Safi, D. Y. Melesse, and A. B. Gumel. Dynamics analysis of a multi-strain cholera model with an imperfect vaccine. *Bulletin of Mathematical Biology*, 75(7):1104–1137, 2013.

[36] Z. Shuai and P. van den Driessche. Global dynamics of cholera models with differential infectivity. *Mathematical Biosciences*, 234(2):118–126, 2011.

[37] V. Singh, R. C. Poonia, S. Kumar, P. Dass, P. Agarwal, V. Bhatnagar, and L. Raja. Prediction of COVID-19 corona virus pandemic based on time series data using support vector machine. *Journal of Discrete Mathematical Sciences and Cryptography*, 23(8), 2020.

[38] G. Q. Sun, J. H. Xie, S. H. Huang, Z. Jin, M. T. Li, and L. Liu. Transmission dynamics of cholera: Mathematical modeling and control strategies. *Communications in Nonlinear Science and Numerical Simulation*, 45:235–244, 2017.

[39] H. R. Thieme. Convergence results and a Poincare-Bendixson trichotomy for asymptotically autonomous differential equations. *Journal of Mathematical Biology*, 30:755–763, 1992.

[40] S. Usaini, A. S. Hassan, S. M. Garba, J. M.-S. Lubuma, A. S. Hassan, S. M. Garba, and J.-s. L. Modeling. Modeling the transmission dynamics of the Middle East Respiratory Syndrome Coronavirus (MERS-CoV) with latent immigrants. *Journal of Interdisciplinary Mathematics*, 26(6):903–930, 2019.

[41] P. van den Driessche. Reproduction numbers of infectious disease models. *Infectious Disease Modelling*, 2(3):288–303, 2017.

[42] K.-M. Wang. Can gold be a safe haven during the COVID-19 pandemic? A quantile causality analysis causality analysis. *Journal of Statistics and Management Systems*, 24(5):1113–1125, 2021.

[43] Y. Wang, J. Liu, and J. M. Heffernan. Viral dynamics of an HTLV-I infection model with intracellular delay and CTL immune response delay. *Journal of Mathematical Analysis and Applications*, 459:506–527, 2018.

[44] Y. Wang and J. Wei. Global Dynamics of a Cholera Model With Time Delay. *International Journal of Biomathematics*, 06(01):125007–1–125007–18, 2012.

[45] Z. Wang and X.-Q. Zhao. Global dynamics of a time-delayed dengue transmission model. *Cana- dian Applied Mathematics Quartelry*, 20(1):89–114, 2012.

[46] H.-m. Wei, X.-z. Li, and M. Martcheva. An epidemic model of a vector-borne disease with direct transmission and time delay. *Mathematical Analysis and Applications*, 342:895–908, 2008.

[47] WHO. Cholera 2014. Weekly Epidemiological Record. Technical Report 40, 2015.

[48] WHO. Weekly Epidemiological Record, 21 September 2018. *Weekly Epidemiological Record*, 93(38):489–500, 2018.

[49] WHO. Cholera Fact Sheets. Technical Report February, 2021.

[50] Z. Xu and X.-Q. Zhao. A vector-bias malaria model with incubation period and diffusion. *Discrete and Continuous Dynamical Systems - Series B*, 17(7):2615–2634, 2012.

[51] X. Zhou, X. Shi, and J. Cui. Stability and backward bifurcation on a cholera epidemic model with saturated recovery rate. *Mathematical Methods in the Applied Sciences*, 40(4):1288–1306, 2016.

[52] X.-y. Zhou and J.-a. Cui. Threshold dynamics for a cholera epidemic model with periodic trans- mission rate. *Applied Mathematical Modelling*, 37:3093–3101, 2013.

[53] X. Y. Zhou, J. A. Cui, and Z. H. Zhang. Global results for a cholera model with imperfect vaccination. *Journal of the Franklin Institute*, 349(3):770–791, 2012.

[54] J. N. Zuckerman, L. Rombo, and A. Fisch. The true burden and risk of cholera: implications for prevention and control. *Lancet Infectious Diseases*, 7:521–530, 2007.

Received November, 2021